The Motion and Active Deformation of India

J. Paul[1], R. Bürgmann[2], V. K. Gaur[1], R. Bilham[3], K. Larson[4], M. B. Ananda[1], S. Jade[1], M. Mukul[1,] T. S. Anupama[1], G. Satyal[5], and D. Kumar[1]

[1] CSIR C-MMACS, NAL Campus, Bangalore 560037, India; [2] Department of Earth and Planetary Science, University of California, Berkeley; [3] CIRES and Department of Geological Sciences, University of Colorado, Boulder; [4] Department of Aerospace Engineering Sciences, University of Colorado, Boulder; [5] G B Pant Institute of Himalayan Environment and Development, Kosi-Katarmal, Almora, India.

Abstract

Measurements of surface displacements using GPS constrain the motion and deformation of India and India-Eurasia plate boundary deformation along the Himalaya. The GPS velocities of plate-interior sites constrain the pole of the angular velocity vector of India with respect to Eurasia to lie at 25.6±1.0°N 11.1±9.0°E, which is located about 6° W of the NUVEL-1A pole of < 3 Ma plate motion. The angular rotation rate of 0.44±0.03° Myr^{-1} is 14 % slower than the long-term rate of 0.51° Myr^{-1}. Insignificant displacements between plate interior sites indicate that the exposed Indian plate is stable to within 7 x 10^{-9} yr^{-1}. About 20 mm/yr of convergence across the Himalaya rotates counterclockwise by about 45° from NW India (~77°E) to E Nepal (~92°E) to remain approximately perpendicular to the Himalayan arc. This rotation of convergence is consistent with E-W extension across southern Tibet.

GPS Velocities

More Details on Data Acquisition and Analysis

GPS data were collected with dual frequency, 9 & 12-channel Trimble 4000 SSE receivers and Trimble SST antennas through 1996, and Trimble 4000 SSI receivers and Dorne Margolin choke ring antennas in more recent occupations. Site occupations commonly lasted three days, and 20 to 24 hours each day. Four types of control-point were used: (a) Concrete Survey of India pillars three feet in height with a circle and a dot on the top surface, (b) a simple circle and dot engraved on bedrock, especially in mountain regions, (c) 1-m^3 concrete cube monoliths flush with the Earth's surface in southern Nepal, and (d) stainless steel pins cemented into rock. XIXth Century triangulation “dots” consist of a ≈1 cm diameter hollowed hemispherical pit supplemented by a fine central mark for GPS work. The time series plots in Figure 1 show when data were collected at individual sites, between 1994 and 1999.

Data for days when there was physical disturbance to the antenna were excluded from the analysis. MIJA was vandalized in 1998 and a new monument was constructed. Data from the new MIJA monument was not used in the analysis. CARI (Andaman Islands) experienced heavy cyclonic winds and thus was disturbed during the 5-day measurement epoch in November 1999. The monument at SHIL (Shillong) was reconstructed by the Survey of India after a first occupation in 1995 leading us to ignore early data from this site. The m_b = 6.3 Chamoli earthquake of March 9, 1999 offset one of our stations, TUNG by 2-3 cm to the southwest. A significantly higher southward rate was observed in the year following the event, presumably

due to accelerated postseismic deformation. We thus include only the pre-earthquake data in our velocity determination for this site.

The data processing at CMMACS relies on the Bernese 4.0 (Bernese Processing Engine) GPS analysis software [Beutler et al., 1996], using precise International GPS Service (IGS) orbits and pole orientation parameters [Beutler et al., 1994]. Station coordinates are computed in the ITRF-96 (International Terrestrial Reference Frame) reference frame by applying tight position constraints to the coordinates of IISC, KIT3, and POL2. ITRF-96 is based on observed velocities at over 200 global geodetic sites with respect to the no-net-rotation NUVEL-1A plate model [Sillard et al., 1998]. All data are processed with a satellite elevation cut-off angle of 15°. For baselines shorter than 500 km we are able to resolve most ambiguities to integer values, whereas for the longer baselines ambiguity resolution is limited. Atmospheric propagation delays are modeled with a zenith delay parameter at each station which is piecewise constant over ~3-hour periods. Average day-to-day repeatabilities of baseline measurements are 3 mm, 8 mm, and 15 mm in the N, E, and vertical components, respectively. We note that the precision in the E component is rather poor, probably due to the difficulty of resolving phase ambiguities. The Nepal GPS data are analyzed using the GIPSY software developed at the Jet Propulsion Laboratory as described in Larson et al. [1999]. The formal coordinate estimation errors from the GPS analyses are multiplied by a factor of 3 (GIPSY solutions) and 5 (Bernese solutions), respectively, to achieve a chi-square per degree of freedom of one in the least squares inversion for station velocities.

Table. GPS station velocities in India reference frame

Longitude	Latitude	E	N	E sigma	N sigma	E-N correl.	Station
(°)	(°)	(mm/yr)	(mm/yr)	(± mm/yr)	(± mm/yr)		
104.316	52.219	-10.94	-43.26	3.70	3.01	-0.01	**IRKT**
74.694	42.680	1.33	-32.96	1.52	1.51	0.00	**POL2**
66.885	39.135	2.70	-33.01	1.40	1.40	0.00	**KIT3**
121.200	31.100	-14.82	-43.34	2.40	2.14	0.00	**SHAO**
78.676	30.997	-7.36	-12.31	2.35	1.46	-0.06	**SUKI**
79.559	30.531	-5.20	-7.26	4.18	2.36	-0.06	**AULI**
79.211	30.486	-11.84	-8.78	3.33	2.19	-0.04	**TUNG**
78.365	30.404	-2.10	-6.99	2.40	1.47	-0.09	**CHAM**
80.194	30.359	-12.00	-13.67	17.57	7.69	-0.19	**BURF**
80.195	30.061	-5.57	0.91	2.50	1.60	-0.06	**MUNS**
81.826	29.967	-4.06	-13.39	1.94	1.24	0.05	**SIMI**
78.680	29.848	-0.56	-4.38	2.89	2.08	-0.04	**LANS**
80.041	29.838	-1.86	-8.60	2.69	1.62	-0.09	**CHAU**
91.104	29.657	4.83	-20.74	2.72	2.43	0.00	**LHAS**
79.620	29.638	1.28	-4.18	4.11	3.04	-0.03	**KTML**
80.148	28.963	-2.90	-0.96	2.00	1.30	0.07	**MAHE**
83.718	28.781	-1.30	-10.44	1.87	1.38	0.04	**JOMO**
87.155	28.630	-1.75	-15.82	4.15	2.10	0.11	**TING**
81.635	28.586	-2.46	-1.64	2.19	1.47	0.06	**SURK**
77.172	28.544	0.80	-3.67	2.52	1.49	-0.04	**JNUC**
83.978	28.199	-0.44	-0.97	2.22	1.48	0.06	**POKH**
86.827	28.194	-1.85	-15.17	5.41	2.51	0.12	**RONG**
81.575	28.134	-1.61	-0.72	1.87	1.24	0.04	**NEPA**

82.573	28.063	-4.70	-1.85	2.25	1.51	0.06	**RANJ**
86.929	27.973	1.20	-9.04	3.73	3.55	0.02	**SCOL**
86.823	27.894	-1.17	-10.43	2.05	1.20	0.05	**PHER**
83.554	27.874	-1.99	-1.54	2.15	1.45	0.04	**TANS**
86.715	27.803	1.35	-8.81	2.05	1.36	0.04	**NAMC**
85.358	27.697	0.13	-2.89	2.16	1.45	0.04	**AIRP**
85.521	27.693	-0.30	-2.27	1.44	1.05	0.02	**NAGA**
86.725	27.683	-0.56	-9.15	2.22	1.34	0.03	**LUKL**
84.430	27.678	-1.25	0.07	2.22	1.47	0.05	**BHAR**
86.230	27.635	-2.00	-6.94	2.19	1.44	0.04	**JIRI**
83.418	27.507	1.36	0.11	2.19	1.48	0.04	**BHAI**
87.206	27.380	2.00	-4.59	2.15	1.39	0.05	**KHAN**
84.982	27.162	-2.30	0.71	2.05	1.27	0.05	**SIMA**
88.503	27.089	-2.46	-5.58	8.47	4.18	-0.31	**DELO**
85.925	26.711	0.77	0.87	2.53	1.48	0.07	**JANK**
87.264	26.484	1.31	1.33	1.79	1.20	0.03	**BIRA**
91.850	25.531	0.88	-6.31	7.60	3.80	-0.08	**SHIL**
77.364	23.284	-1.90	-9.99	4.76	3.50	-0.05	**BHOP**
74.936	13.057	5.99	1.17	5.50	2.57	0.05	**MIJA**
76.970	13.025	-0.13	-0.01	2.76	1.32	-0.02	**RANG**
77.570	13.021	-1.47	-1.40	1.00	1.00	0.00	**IISC**
78.515	12.952	-1.01	0.27	2.54	1.31	-0.03	**KRIS**
80.176	12.927	-0.18	-0.58	2.98	1.60	-0.03	**NANM**
77.626	12.625	-0.29	0.49	4.39	1.93	-0.01	**DEVA**
92.719	11.613	-12.52	-4.53	3.36	2.03	-0.02	**CARI**
77.587	11.157	0.89	1.12	2.60	1.49	-0.05	**CHEN**
76.816	10.825	3.35	-0.68	6.49	2.99	0.00	**PLGT**
78.462	10.656	1.07	-0.88	5.95	3.02	-0.05	**MANA**
77.556	10.428	6.42	1.19	8.38	4.47	-0.01	**PLNI**
77.465	10.232	6.05	0.44	14.90	7.81	-0.05	**KODI**
77.677	8.183	0.67	5.19	2.51	1.58	-0.02	**PONN**

Related Figures

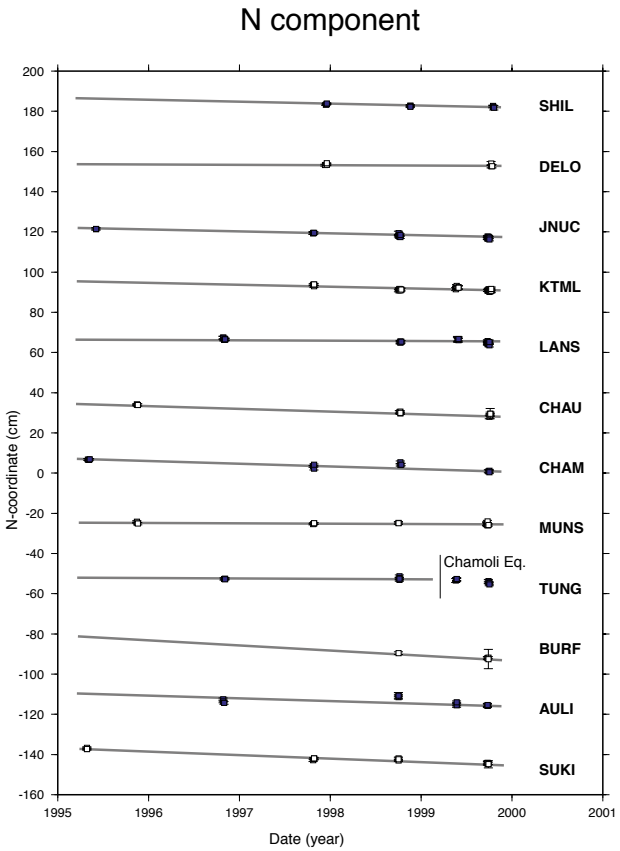

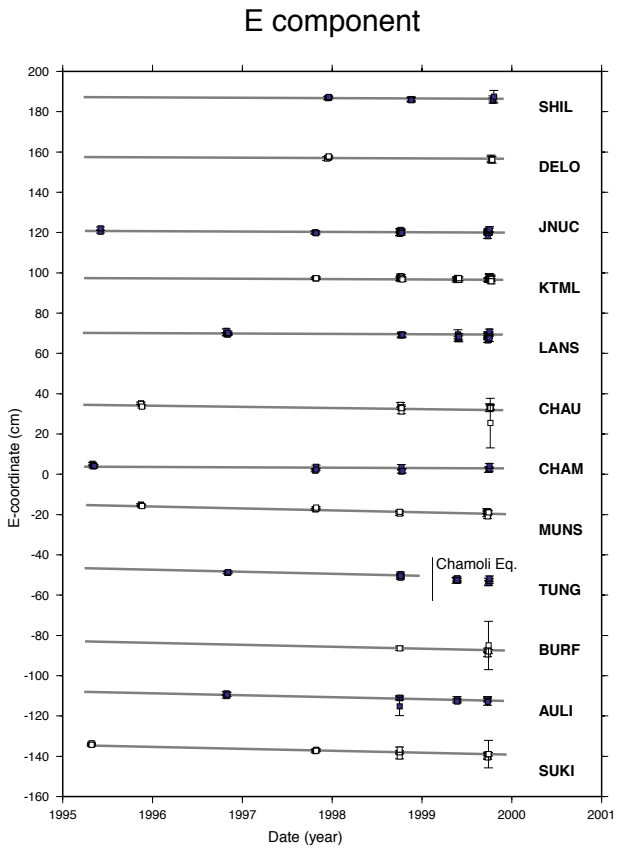

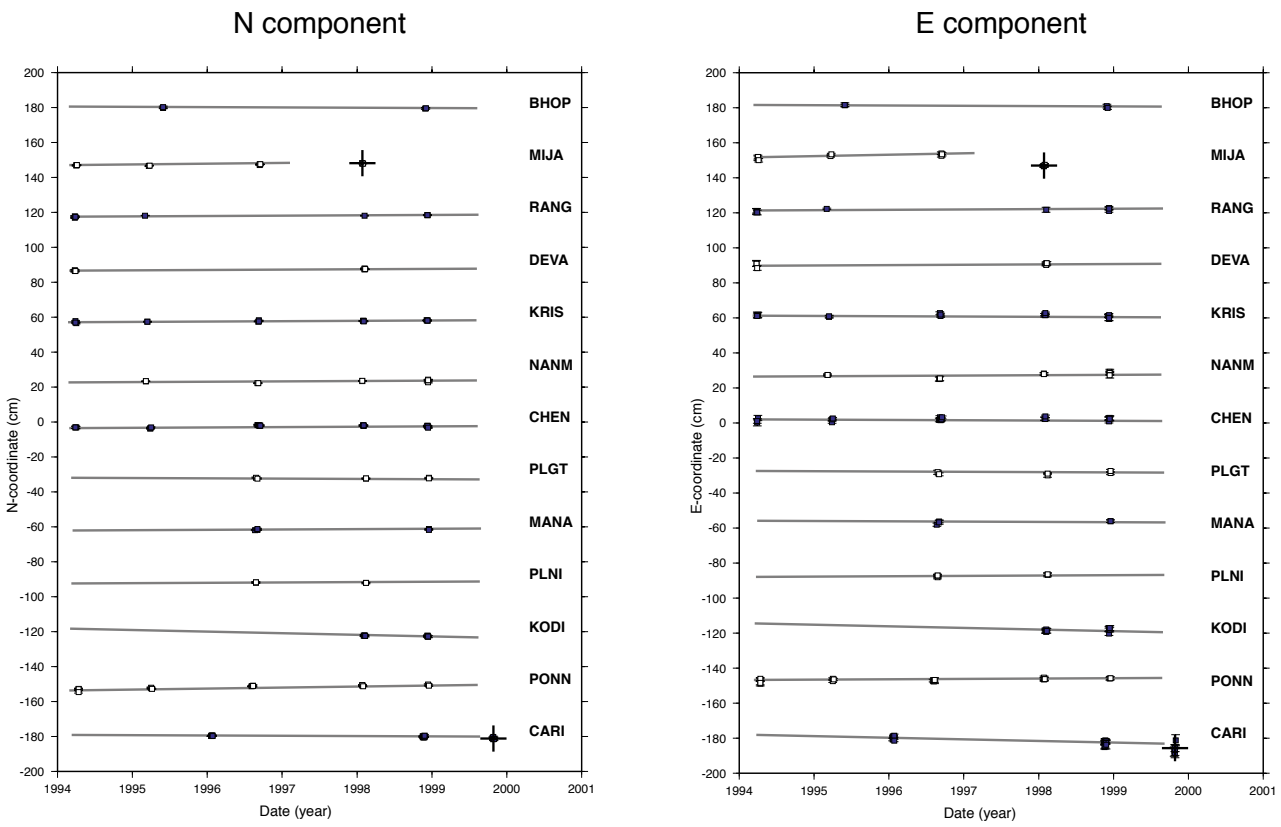

Figure A (a) North and east coordinate time series plots of Himalayan stations relative to IISC, Bangalore. (b) Time series of north and east coordinates of Indian subcontinent stations and site on Andaman Islands (CARI) relative to IISC. The time series are offset and alternating solid and filled symbols are used for clarity. The vertical units are in cm. Note that the Himalaya occupations were initiated in 1995, whereas the first GPS survey of the southern Trigon occurred in 1994.

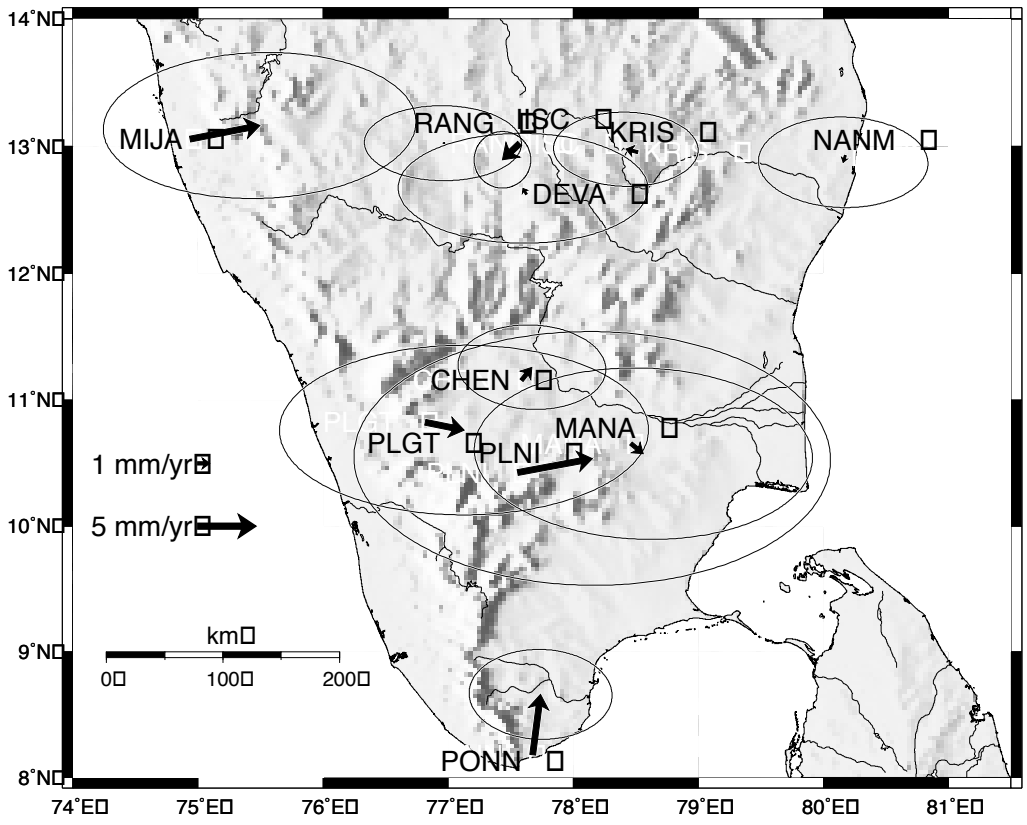

Figure B Close up of GPS velocities of the southern Trigon network on shaded relief map. All but one velocity are insignificantly different from zero motion.